

NWP SAF

Satellite Application Facility for Numerical Weather Prediction

Document NWPSAF-KN-TR-008

Version 1.1



04-04-2013

How to calculate wind spectra

Jur Vogelzang

KNMI, De Bilt, The Netherlands



		How to calculate wind spectra	Doc ID : NWPSAF-KN-TR-008 Version : 1.1 Date : 25-03-2013
--	--	--------------------------------------	---

How to calculate wind spectra

Jur Vogelzang

KNMI, The Netherlands



This documentation was developed within the context of the EUMETSAT Satellite Application Facility on Numerical Weather Prediction (NWP SAF), under the Cooperation Agreement dated 29 June 2011, between EUMETSAT and the Met Office, UK, by one or more partners within the NWP SAF. The partners in the NWP SAF are the Met Office, ECMWF, KNMI and Météo France.

Copyright 2012, EUMETSAT, All Rights Reserved.

Change record			
Version	Date	Author / changed by	Remarks
0.1	July 2010	Jur Vogelzang	First draft
1.0	July 2010	Jur Vogelzang	First public version
1.1	March 2013	Jur Vogelzang	Corrected some errors in chapter 2 pointed out by Marcos Portabella

Contents

1	Introduction	5
1.1	Background	5
1.2	Aims and scope	5
1.3	Introductory remarks	5
2	The wind spectrum	7
2.1	Definitions	7
2.2	Sampling method	10
2.3	Moments method	10
2.4	Wind spectrum	12
2.5	Resume	12
2.6	A note on the orthogonality relation	13
3	Method of calculation	15
3.1	Data	15
3.2	Detrending	15
3.3	Variance	20
3.4	Multitapering	21
3.5	Comparison of sampling and moments methods	23
3.6	Sampling strategy	24
4	Conclusions	29
	References	31
	Appendix A Finite differencing	33

		How to calculate wind spectra	Doc ID : NWPSAF-KN-TR-008 Version : 1.1 Date : 25-03-2013
--	--	--------------------------------------	---

1 Introduction

1.1 Background

Spectra of the wind vector components are an important tool for assessing the spatial characteristics of atmospheric motions. This holds in particular when measurements at regular distances are available, as is the case for measurements from aircraft [*Nastrom et al.*, 1984; *Nastrom and Gage*, 1985] or space-borne scatterometers. The latter constitute the only data source for global ocean surface vector winds.

Within the framework of the Satellite Application Facility for Numerical Weather Prediction (NWP SAF) wind spectra were studied earlier [*Vogelzang*, 2006] following an approach based on autocorrelation of the wind speed components over all available wind data. However, the results obtained in this study were not compatible with those obtained by other authors, e.g., [*Freilich and Chelton*, 1986; *Patoux and Brown*, 2001; *Chelton et al.*, 2006]. After discussion in the Ocean Vector Wind Science Team (OVWST) it was decided to revisit the problem of calculating spectra from scatterometer winds

The new study tackled the problem in a broader approach. It was found that the method used by *Vogelzang* [2006] was not correct: it effectively used box sampling resulting in a k^{-2} contribution to the spectrum that dominates at high spatial frequencies. Moreover, it was shown that a sample-based approach leads to correct spectra, as long as the effect of wind features larger than the sample size is filtered out in the appropriate way (detrending). The resulting spectra agree very well with those obtained by others and show no residual artefacts..

1.2 Aims and scope


This report is intended as a “cook-book” with recipes for calculating spectra of scatterometer winds. The methods developed in this reports can be applied to all other wind measurements on regular intervals, like aircraft measurements.

Further analysis of the wind spectra as well as their application, for instance in the calculation of representation errors in the triple collocation method, will be described in other reports and/or publications, e.g., [*Vogelzang et al.*, 2010].

1.3 Introductory remarks



Chapter 2 summarizes the theory for calculating spectra from measurements on a regular grid. This material can be found in many text books, e.g., *Press et al.* [1986], *Percival and Walden* [1993] but it is included here for the sake of completeness.

Chapter 3 contains the results of this study. After introduction of the data used in section 3.1 the various detrending methods are described in detail. It is shown that application of a linear transformation that maps

<p>The EUMETSAT Network of Satellite Application Facilities</p>		<h2>How to calculate wind spectra</h2>	<p>Doc ID : NWPSAF-KN-TR-008 Version : 1.1 Date : 25-03-2013</p>
---	---	--	--

both end points of the sample to the same value, first differencing, or windowing with a normalized window function yields good results. The multitaper method, a generalization of the windowing method, yields good results if the number of individual spectra happens to be small. It is shown that the sampling and moment methods for calculating individual spectra are identical, as expected. Interpolation of isolated gaps greatly increases the number of available samples in case of scatterometer data. The sample size can not be increased without limit, because the number of available samples decreases rapidly with the sample size.

The report end with conclusions in chapter 4. Some technical information is given in the Appendix.

		How to calculate wind spectra	Doc ID : NWPSAF-KN-TR-008 Version : 1.1 Date : 25-03-2013
--	--	--------------------------------------	---

2 The wind spectrum

Given a sample of N wind measurements at regular distances, the spectrum is calculated as the periodogram of the sample (also referred to as the individual spectrum). This can be done in two equivalent ways:

1. The **sampling method**: Fourier transform the sample with an FFT algorithm and take the square of the absolute value of each frequency component.
2. The **moments method**: Calculate the mixed second order moment (or autocorrelation) and Fourier transform with an FFT algorithm.

Unfortunately, the periodogram is very noisy: the expectation value of the error in a periodogram estimate equals the value of that estimate itself [Press *et al.*, 1986; Percival and Walden, 1993]. Therefore more samples are needed so that an average can be made of the periodograms from each sample. This can also be achieved by breaking a long sample of L measurements into K samples of length N . If K is the number of samples, the relative error in each component of the averaged spectrum equals $K^{-1/2}$.

This chapter gives the relevant definitions and formulas for both methods, and establishes the relation between them by relating the spectra obtained with these methods to the variance of the wind field.

2.1 Definitions

Fourier transform



In the continuous case, the Fourier transformation between a wind component $u(x)$ in the spatial domain and $U(k)$ in the spatial frequency domain reads [Press *et al.*, 1988]

$$U(k) = \int_{-\infty}^{\infty} dx e^{2\pi i k x} u(x) \quad , \quad (1a)$$

$$u(x) = \int_{-\infty}^{\infty} dk e^{-2\pi i k x} U(k) \quad , \quad (1b)$$

where $k = 1/x$.

These equations can be discretized for the case that $u_j = u(x_j)$ is sampled on a regular grid with size Δ , so $x_j = j\Delta$, $j = 0, 1, \dots, N-1$. The FFT algorithm prescribes that the spatial frequency is restricted to a regular grid with size $(N\Delta)^{-1}$ and spatial frequencies $k_l = l(N\Delta)^{-1}$, $l = -N/2, \dots, N/2$. The discretized Fourier transform reads

		<h2 style="text-align: center;">How to calculate wind spectra</h2>	Doc ID : NWPSAF-KN-TR-008 Version : 1.1 Date : 25-03-2013
--	--	--	---

$$U_l = U(k_l) = \Delta \sum_{j=0}^{N-1} \exp\left(2\pi i \frac{jl}{N}\right) u_j \quad , \quad (2a)$$

$$u_j = u(x_j) = \frac{1}{N\Delta} \sum_{l=0}^{N-1} \exp\left(-2\pi i \frac{jl}{N}\right) U_l \quad , \quad (2b)$$

where we used the fact that the exponential is periodic to redefine the range of values of the index l .

The FFT algorithm works only on the summations in (2a) and (2b) and not on the factor in front of them. Denoting the input of the FFT algorithm with u_j and its output with \hat{u}_l (or vice versa when considering the inverse FFT) one obtains

$$\hat{u}_l = \sum_{j=0}^{N-1} \exp\left(2\pi i \frac{jl}{N}\right) u_j \quad , \quad (3a)$$

$$u_j = \frac{1}{N} \sum_{l=0}^{N-1} \exp\left(-2\pi i \frac{jl}{N}\right) \hat{u}_l \quad . \quad (3b)$$

Now the grid size has disappeared, but the factor $1/N$ in the inverse transformation remains. Note that $U_l = \hat{u}_l \Delta$.

Moments and variance

The average or first moment of the wind field reads

$$\langle u \rangle = \frac{1}{N} \sum_{j=0}^{N-1} u_j \quad , \quad (4a)$$

and the second moment reads



$$\langle u^2 \rangle = \frac{1}{N} \sum_{j=0}^{N-1} u_j^2 \quad . \quad (4b)$$

Note that the sampled values are numbered from zero rather than from one, to keep in line with the conventions used in the FFT algorithm. The total variance of the wind field is defined as

$$\sigma^2 = \langle u^2 \rangle - \langle u \rangle^2 \quad . \quad (5)$$

If the average or first moment is zero, the variance becomes equal to the second moment. In case of the zonal and meridional wind components (u, v) the first moment is much smaller than second moment but can not be neglected.

From (3a) one easily infers that $\hat{u}_0 = N \langle u \rangle$.

		How to calculate wind spectra	Doc ID : NWPSAF-KN-TR-008 Version : 1.1 Date : 25-03-2013
--	--	--------------------------------------	---

Mixed second order moment

The second order moment for distance $j\Delta$, $j = 0, \dots, N-1$, reads

$$a_j = \frac{1}{M} \sum_{m=0}^{M-j-1} u_m u_{m+j} \quad , \quad (6)$$

where M is the total number of points in the dataset. For good statistics one should have $M \gg N$. Note that $a_0 = \langle u^2 \rangle$. The quantity a_j in (6) is also referred to as autocorrelation or covariance. This is not strictly true, since the covariance is corrected for the average values and the autocorrelation equals the covariance normalized to one at zero lag.

Spectrum

In the continuous case the spectrum ψ in the spatial frequency domain is defined such that

$$\int_{-\infty}^{\infty} dk \psi(k) = \sigma^2 \quad , \quad (7)$$



so that the integral over ψ in the spatial frequency interval (k_1, k_2) can be interpreted as the variance in that interval. Equation (7) can not be converted directly to the discrete case, but should be modified to, see also (4b),

$$\frac{1}{N\Delta} \sum_{l=0}^{N-1} \psi_l = \langle u^2 \rangle \quad . \quad (8a)$$

The discrete spectral component ψ_0 or the continuous value $\psi(0)$ is proportional to the average value of u . However, $\psi(0)$ has measure zero in (7), while ψ_0 has a measure $(N\Delta)^{-1}$ (which goes to zero when N approaches infinity). To relate the spectrum in the discrete case to the variance one may remove the average (bias) from each sample. This procedure yields $\psi_0 = 0$ and leaves the other values ψ_l , $l = 1, \dots, N$ unaffected. One may also modify (8a) to

$$\frac{1}{N\Delta} \sum_{l=1}^{N-1} \psi_l = \sigma^2 \quad . \quad (8b)$$

Note that the spectrum is generally plotted as a function of the spatial frequency, so the factor $(N\Delta)^{-1}$ in (8a-b) must be taken into account to retain proper scaling. If the spectrum were plotted as a function of the index l this would not be necessary. The dimension of the spectrum is m^3/s^2 .

		How to calculate wind spectra	Doc ID : NWPSAF-KN-TR-008 Version : 1.1 Date : 25-03-2013
--	--	--------------------------------------	---

2.2 Sampling method

Consider a single sample of length N . When the samples are properly corrected for the average, the total variance follows from (4b) as

$$\langle u^2 \rangle = \frac{1}{N} \sum_{j=0}^{N-1} u_j^2 \quad .$$

Expressing the wind values u_j in terms of their FFT coefficients \hat{u} according to (3b), with u the input to the FFT algorithm and \hat{u} the output, yields

$$\begin{aligned} \langle u^2 \rangle &= \frac{1}{N} \sum_{j=0}^{N-1} \left(\frac{1}{N} \sum_{l=0}^{N-1} \exp\left(-2\pi i \frac{jl}{N}\right) \hat{u}_l \right) \left(\frac{1}{N} \sum_{m=0}^{N-1} \exp\left(-2\pi i \frac{jm}{N}\right) \hat{u}_m \right)^* = \\ &= \frac{1}{N^3} \sum_{l,m=0}^{N-1} \hat{u}_l \hat{u}_m^* \sum_{j=0}^{N-1} \exp\left(-2\pi i \frac{j(l-m)}{N}\right) = \\ &= \frac{1}{N^3} \sum_{l,m=0}^{N-1} \hat{u}_l \hat{u}_m^* N \delta_{l-m,0} = \\ &= \frac{1}{N^2} \sum_{l=0}^{N-1} |\hat{u}_l|^2 \quad , \end{aligned} \tag{9}$$

with $\delta_{j,n}$ the Kronecker delta which equals 1 if $j = n$ and zero elsewhere. Combining with (8a) gives

$$\frac{1}{N\Delta} \sum_{l=0}^{N-1} \psi_l = \frac{1}{N^2} \sum_{l=0}^{N-1} |\hat{u}_l|^2 \quad , \tag{10}$$

so the final result is



$$\psi_l = \frac{\Delta}{N} |\hat{u}_l|^2 \quad . \tag{11}$$

Equation (11) gives the relation between the spectrum and the FFT output for the sampling method.

2.3 Moments method

Consider again a single sample of length N . In addition, assume that the sample is periodic, so all indices should be taken modulo $N - 1$. The FFT output of the mixed second order moments is (see 3a)

$$\begin{aligned} \hat{a}_l &= \sum_{j=0}^{N-1} \exp\left(2\pi i \frac{jl}{N}\right) a_j = \\ &= \frac{1}{N} \sum_{j=0}^{N-1} \exp\left(2\pi i \frac{jl}{N}\right) \sum_{m=0}^{N-1} u_m u_{m+j} \quad , \end{aligned} \tag{12}$$

		How to calculate wind spectra	Doc ID : NWPSAF-KN-TR-008 Version : 1.1 Date : 25-03-2013
--	--	--------------------------------------	---

where the definition of the mixed second order moment (6) has been used, with the modification that the sample is now periodic with length N . Replacing the coefficients u by their FFT counterparts according to (3b) yields

$$\begin{aligned}
\hat{a}_l &= \frac{1}{N} \sum_{j=0}^{N-1} \exp\left(2\pi i \frac{jl}{N}\right) \sum_{m=0}^{N-1} \frac{1}{N} \sum_{p=0}^{N-1} \exp\left(-2\pi i \frac{mp}{N}\right) \hat{u}_p \frac{1}{N} \sum_{q=0}^{N-1} \exp\left(-2\pi i \frac{(m+j)q}{N}\right) \hat{u}_q = \\
&= \frac{1}{N^3} \sum_{p,q=0}^{N-1} \hat{u}_p \hat{u}_q \sum_{j=0}^{N-1} \exp\left(2\pi i \frac{j(l-q)}{N}\right) \sum_{m=0}^{N-1} \exp\left(-2\pi i \frac{m(p+q)}{N}\right) = \\
&= \frac{1}{N^2} \sum_{p,q=0}^{N-1} \hat{u}_p \hat{u}_q \sum_{j=0}^{N-1} \exp\left(2\pi i \frac{j(l-q)}{N}\right) \delta_{p+q,0} = \\
&= \frac{1}{N^2} \sum_{p=0}^{N-1} \hat{u}_p \hat{u}_{-p} \sum_{j=0}^{N-1} \exp\left(2\pi i \frac{j(l+p)}{N}\right) = \\
&= \frac{1}{N} \sum_{p=0}^{N-1} \hat{u}_p \hat{u}_{-p} \delta_{l+p,0} = \\
&= \frac{1}{N} \hat{u}_l \hat{u}_{-l} \quad .
\end{aligned} \tag{13}$$

Note that the sample is considered as periodic, so its final point forms a pair with lag size 1 with its first. Since $\hat{u}_{-l} = \hat{u}_l^*$ equation (13) reduces to

$$\hat{a}_l = \frac{1}{N} |\hat{u}_l|^2 \quad . \tag{14}$$

Comparison of (14) with (9) yields

$$\langle u^2 \rangle = \frac{1}{N} \sum_{l=0}^{N-1} \hat{a}_l \quad , \tag{15}$$



and comparison with (8) gives the final result

$$\psi_l = \hat{a}_l \Delta \quad . \tag{16}$$

Note that the Fourier transform of the mixed second order moments should be real and even, since the moments themselves are real and even. Note also that (14) and (16) yield (11), so the sampling method and the moments method give the same spectrum, provided that the samples are considered periodic.

2.4 The wind spectrum

The spectrum with components ψ_l is defined for positive and negative spatial frequencies and satisfies the normalization condition (8). This can be written as

		How to calculate wind spectra	Doc ID : NWPSAF-KN-TR-008 Version : 1.1 Date : 25-03-2013
--	--	--------------------------------------	---

$$\langle u^2 \rangle = \frac{1}{N\Delta} \left(\psi_0 + \sum_{l=1}^{N/2-1} \psi_l + \psi_{N/2} + \sum_{m=N/2+1}^{N-1} \psi_m \right) = \frac{1}{N\Delta} \left(\psi_0 + \sum_{l=1}^{N/2-1} (\psi_l + \psi_{N-l}) + \psi_{N/2} \right) , \quad (17)$$

where the substitution $m \rightarrow N-l$ has been made to combine the summations. This can be written in terms of the one-sided spectral density Ψ as

$$\langle u^2 \rangle = \frac{1}{N\Delta} \sum_{l=0}^{N/2} \Psi_l , \quad \sigma^2 = \frac{1}{N\Delta} \sum_{l=1}^{N/2} \Psi_l , \quad (18)$$

where

$$\begin{aligned} \Psi_0 &= \psi_0 , \\ \Psi_l &= \psi_l + \psi_{N-l} , \quad l = 1, 2, \dots, \frac{N}{2} - 1 , \\ \Psi_{N/2} &= \psi_{N/2} . \end{aligned} \quad (19)$$

The one-sided spectral density Ψ will further be referred to as the wind spectrum.

2.5 Resume

The relation between the output of the FFT algorithm and the spectrum is



$$\Psi_l = \begin{cases} \frac{\Delta}{N} |\hat{u}_0|^2 \\ \frac{\Delta}{N} (|\hat{u}_l|^2 + |\hat{u}_{N-l}|^2) , \quad l = 1, 2, \dots, N/2 , \quad \text{for the sampling method,} \\ \frac{\Delta}{N} |\hat{u}_{N/2}|^2 \end{cases} \quad (20a)$$

$$\Psi_l = \begin{cases} \Delta \hat{a}_0 \\ \Delta (\hat{a}_l + \hat{a}_{N-l}) , \quad l = 1, 2, \dots, N/2 , \quad \text{for the moments method,} \\ \Delta \hat{a}_{N/2} \end{cases} \quad (20b)$$

where \hat{u} and \hat{a} are the output coefficients of the FFT algorithm with as input the sampled wind components and the mixed second order moments, respectively. The spectrum Ψ is defined in such a way that the total variance is given by

$$\sigma^2 = \frac{1}{N\Delta} \sum_{l=1}^{N/2} \Psi_l . \quad (21)$$

When plotted as a function of k , the area under Ψ in an interval (k_1, k_2) equals the variance in that interval, assuming only nonnegative values for k . The spectrum is expressed in units of m^3/s^2 . The domain of Ψ is $[0, k_{\max}]$ with

		How to calculate wind spectra	Doc ID : NWPSAF-KN-TR-008 Version : 1.1 Date : 25-03-2013
--	--	--------------------------------------	---

$$k_{\max} = \frac{1}{2\Delta} \quad . \quad (22)$$



2.6 A note on the orthogonality relation

The results in sections 2.3 and 2.4 were derived using the orthogonality relation

$$\sum_{j=0}^{N-1} \exp\left(2\pi i \frac{jn}{N}\right) = N\delta_{n,0} \quad . \quad (23)$$

It is easy to show that this holds for $n = 0$: each term in the summation equals 1, so the sum adds up to N . For $n \neq 0$ the terms of (23) lie on the unit circle in the complex plane. The terms form a regular pattern of points with equal angular distance between neighbors. Summing all contributions is the same as taking N times the average, which is of course zero.

It is also straightforward to show that (23) holds numerically to machine precision. Since the right hand side of (23) is real, the relation also holds with a minus sign in the exponential.

		How to calculate wind spectra	Doc ID : NWPSAF-KN-TR-008 Version : 1.1 Date : 25-03-2013
--	--	--------------------------------------	---

3 Method of calculation

3.1 Data

The results obtained in this section were obtained from all SeaWinds data from January 2008. These data were processed with the SeaWinds Data Processor (SDP) version 2.0 at 25 km resolution, using two dimensional variational ambiguity removal (2DVAR) with the ECMWF prediction as background. Outer swath processing was included and variational quality control was switched off, though wind vector cells (WVC's) contributing more than 12 to the observation cost function were flagged with the variational quality control (VQC) flag. WVC's with the VQC flag or the Maximum Likelihood estimator (MLE) flag set were excluded for processing. The MLE flag indicates the presence of rain, ice, or extreme wind variability in the WVC..

The samples for calculating the spectrum or the mixed second order moments were taken along the satellite moving direction (fixed WVC number). Single missing values were filled by default using linear interpolation; larger holes in the data caused the sample to be rejected.

The default sample size was 128 points, spanning 3200 km; the mixed second order moments were calculated for 64 lags. Since the mixed second order moments are symmetrized before calculating the Fourier transform, the spectra obtained for the two methods have the same size and are therefore defined on the same grid of spatial frequencies.

The spectra are plotted against the spatial frequency k which is the inverse of the distance, so $k = 10^{-5} \text{ m}^{-1}$ corresponds to a distance of 10^5 m , or 100 km.

3.2 Detrending

The Earth's surface wind field contains large scale structures like the trades in the subtropics and cyclones in the extratropics. To sample such large scales one needs large sample sizes, otherwise the wind may differ considerably between the first and last point of the sample, and such a difference will cause a k^{-2} contribution to the spectrum since the sample is considered periodic. However, such large sample sizes are not possible in practice for scatterometer winds due to gaps in the data caused by land, rain, and sea ice. Detrending is a technique for obtaining good spectral estimates for relatively small samples.

One can identify three methods for detrending:

- **Subtraction method:** subtraction of a linear function representing the long scales not resolved by the sample [Errico, 1985; Frehlich and Sharman, 2008];
- **First differencing:** taking the first difference of each sample. This is a linear high pass filtering operation with known spectral response [Percival and Walden, 1993];

- **Windowing:** multiplying with a windowing function that maps both ends of the sample to zero [Press *et al.*, 1988].

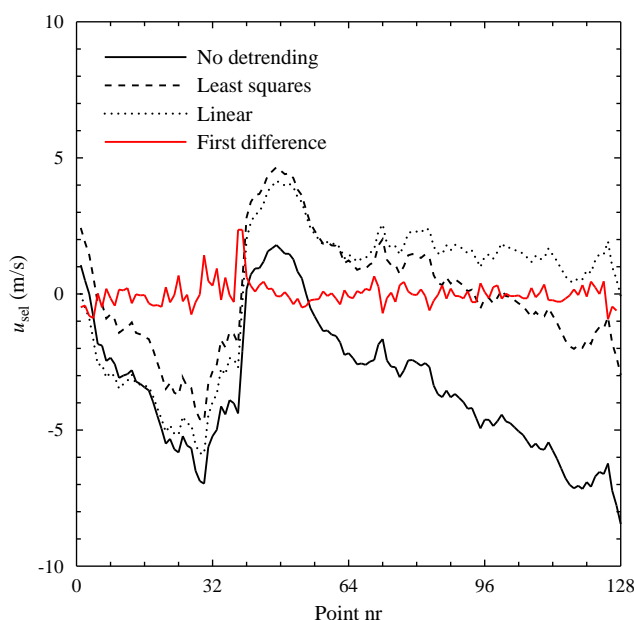


Figure 3.1 Effect of various detrending methods on the first sample of the zonal wind component u .

Figure 3.1 shows the zonal wind component u for the first sample encountered in the dataset. The black solid curve shows the original sample. As can be seen from figure 3.1 there is a jump of 10 m/s between the first and last point of the sample. This jump is much larger than that between any other neighbouring points in the sample. The dashed and dotted black curves show the result of two variants of the subtraction method: subtraction of a least squares fit (dashed) and subtraction of a linear function such that both end points of the sample get value zero (dotted). The dashed curve shows some difference at the ends, the dotted curve not (by definition). Finally, the solid red curve shows the result of first differencing. Now all medium to large scale is filtered out.

The high pass filtering in the first differencing method can easily be corrected for in the spectral domain to yield the correct variance as shown in appendix A. Windowing can be considered as the Fourier transform of first differencing: a suitable window function may transform to a linear filter in the spectral domain which may be inverted to retrieve the variance of the original signal. However, a given window function is not guaranteed to transform into a linear filter. In fact, most popular window functions will not.

Subtraction method

Figure 3.2 shows the spectra for the wind components u and v obtained with the two variants of the subtraction method described above. The blue curves pertain to the wind components measured with the scatterometer, the red curves to those of the background (model).

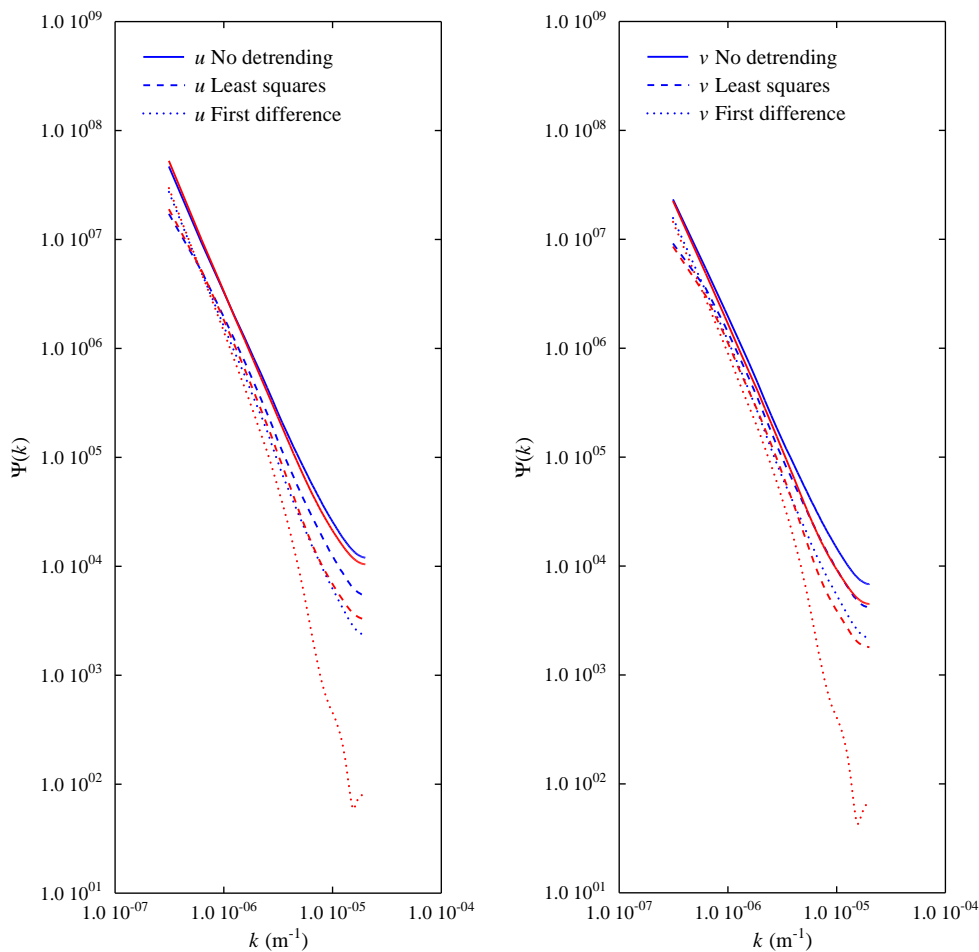


Figure 3.2 Spectra for the wind components u (left) and v (right) of the scatterometer wind (blue) and the model wind (red) obtained with various subtraction detrending methods.

Without detrending the spectra have a k^{-2} behaviour with noise flattening the spectra towards high spatial frequencies. The model spectrum is slightly below the observation spectrum, somewhat more pronounced for v , just like observed earlier [Vogelzang, 2006]. Figure 3.2 shows that detrending with the linear transformation reduces the spectrum considerably, especially for the model wind at high spatial frequencies. Least squares detrending has a less pronounced effect. This agrees with the findings from figure 3.1: subtraction of a least squares fit from each sample may still leave a considerable jump between the first and last point of the sample. Subtraction of a linear function that maps both ends to zero does not cause such a jump by definition

First differencing

As can be seen from figure 3.1, first differencing acts like a high-pass filter. The spectra shown in figure 3.3 are corrected for this using the first difference transfer function (see appendix A).

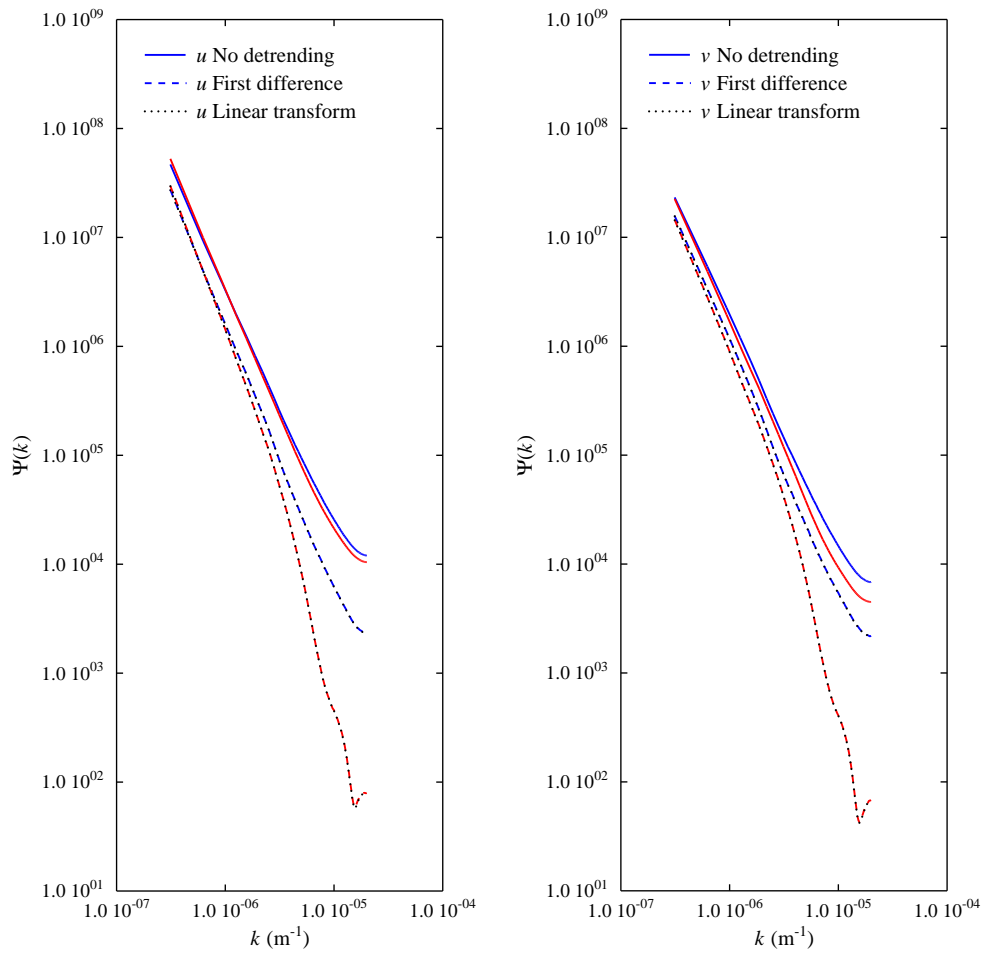


Figure 3.3 Spectra obtained for first differencing (dashed) and linear transformation (black dotted).

The black dotted lines in figure 3.3 are obtained with the linear transformation and are identical to the dotted curves in figure 3.2. The results for first differencing and linear transformation coincide on the scale of figure 3.3. Inspection of the numerical results shows that the spectral densities obtained with first differencing are slightly higher, by about 1%, than those obtained with the linear transformation.

Windowing

Another method to force the end points at each sample to zero is to apply a window function to the samples [Press et al., 1987]. Such a function is zero at the end points and normalized as [Percival and Walden, 1993]

$$\sum_{i=1}^N h_i^2 = 1 \quad , \quad (25)$$

where h_i is the window function value at point i of the sample, $i = 1, \dots, N$.

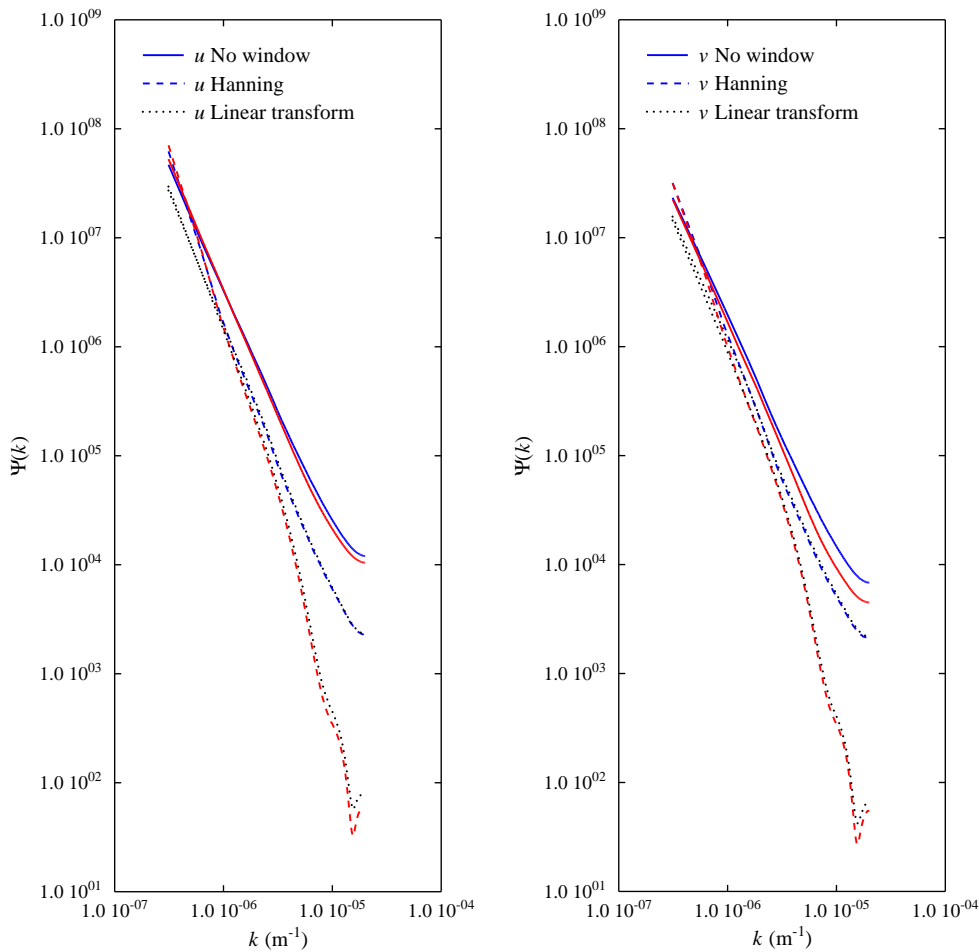




Figure 3.4 Spectra for the wind components u (left) and v (right) without windowing (solid curves) and with the Hanning window (dashed curves). The dotted curves show the linear transformation result as a reference.

Figure 3.4 shows the effect of the Hanning window. The Parzen, and Welch windows give almost the same results, indiscernible from each other in the scale of the figure, and are therefore not shown. The dotted curves show the linear transformation result from the previous figures as a reference.

Note the similarity between figures 3.4 and 3.2-3.3: the solid curves are without windowing or detrending and are identical for both figures while the dashed curves in figure 3.4 (Hanning window) closely resembles the dot-dashed and dotted curves in figure 3.3 (first difference and linear transformation, respectively). It is easily understood why windowing should have an effect similar to the linear transformation: windowing also forces the end points of each sample to zero. The largest differences are at the first two nonzero frequencies where the Hanning window yields spectral densities that are larger by a factor of 2.3 and 1.5, respectively, than the corresponding densities obtained with the linear transformation.

The spectra for the transversal and longitudinal wind components, τ and λ , respectively bear close resemblance with those of u and v (no results shown). This is as expected since most of the scatterometer

		<h1>How to calculate wind spectra</h1>	Doc ID : NWPSAF-KN-TR-008 Version : 1.1 Date : 25-03-2013
--	--	--	---

observations are made in cases where (τ, λ) differs little from (u, v) . The main difference is a sign change in descending orbits, but this does not affect the spectrum.

3.3 Variance

As stated earlier, the rationale behind detrending is that the wind field contains features on scales much larger than the sample size which is typically 3200 km. These features are therefore not represented in the spectra. However, they do cause a trend in the sampled signal. In first order this trend can be considered as linear, giving a saw-tooth shaped contribution to the sampled signal. When considered as a periodic function, the saw-tooth has a k^{-2} spectrum [Wikipedia, 2009] that dominates the wind spectrum, especially at high frequencies and for the model spectrum, because the model spectral density is very low there. Removing the saw-tooth for each separate sample by detrending, reveals the subtle details in the spectrum as shown in figures 3.2 – 3.4.

However, detrending also has a disadvantage: because the sampled signal is manipulated, the spectrum no longer needs to be properly normalized to the total variance. In fact, this correspondence is destroyed when the spectrum is averaged over two or more samples because each spectrum gives the variance with respect to the sample average, but when two spectra are averaged, the total variance of the two samples together is not equal to the average of the variances over the individual samples. This is due to the fact that the average enters the variance equation (5) quadratically.

This can also be visualized by assuming two samples, each with small variance $\sigma^2 \ll 1$. Suppose one sample has average +1 and the other -1. When the sample variances are averaged, the result will still be σ^2 , but when the two samples are combined to one data set the variance of this set will be much larger than σ^2 .

Table 3.1 shows the total variance, obtained directly from the samples and calculated from the spectra obtained with different methods for detrending. The directly obtained variances are given in the first two rows of table 3.1. The first row, labelled “Direct” gives the total variance over the complete dataset; the second row, labelled “De-averaged” is obtained by subtracting the average from each sample, thus giving the average of the variances in each individual sample rather than that of the whole data set. Table 3.1 shows that this yields a difference of about a factor 2.

As can be seen from table 3.1, the subtraction and filtering detrending methods suffer from a significant loss of variance of a factor of about 2 compared to the de-averaged raw samples. Most variance is lost by the least squares method, while the linear transform and first differencing methods give similar results. The windowing methods come much closer to the de-averaged variance. This is no surprise, since windowing yields larger values for the spectral density at small frequencies than subtraction or filtering, and the low frequencies contain most of the variance.

Method	Type	Sel u	Sel v	Mod u	Mod v
No	Direct	41.478	23.429	46.362	23.142
	De-averaged	21.134	11.061	23.032	10.279
Subtraction	Least squares	9.053	5.460	9.307	4.728
	Linear transform	11.547	7.053	11.898	6.135
Filtering	First differencing	11.594	7.094	11.951	6.168
Windowing	Hanning	23.247	12.674	25.629	12.121
	Parzen	22.015	11.895	24.201	11.281
	Welch	20.846	11.250	22.846	10.580

Table 3.1 Variances for the scatterometer (Sel) and model (Mod) wind components u and v in m^2/s^2 obtained directly from the samples or from the spectra obtained with various detrending options.

Windowing causes some loss of variance near the edges of the sample, but this is compensated by overcounting the variance in the middle of the sample because of the normalisation condition (24). The Parzen and Welch windows yield the variances closest to the average variance of the de-averaged samples.

The spectra in figures 3.2 - 3.4 show that most of the variance is contained in the lowest spatial frequencies (largest spatial scales) and that the high frequency part of the spectrum is almost the same for the windowing methods, the first difference method, and the linear transformation subtraction method. It is therefore concluded that these methods yield reliable values for the wind spectrum at mid and high spatial frequencies.

3.4 Multitapering

Multitapering can be considered as an extension to the windowing method. The spectrum is given by

$$\Psi(k) = \frac{1}{M} \sum_{m=1}^M \Psi_m(k) \quad , \quad (26)$$

where Ψ_m is obtained from the sample with the multitaper function of order m as window. The multitaper function values are discrete prolate spheroidal sequences (DPSS). The maximum order M is related to the width of the multitaper and restricted to small numbers, see *Percival and Walden* [1993] for more information.

Figure 3.5 shows the multitaper functions of order 1 to 4 for a width equal to twice the frequency resolution on a grid of 128 points. The first order window looks very much like a Hanning window. Note that the higher order multitaper functions take more and more of the sample at its ends into account.

Figure 3.6 shows the spectra resulting from application of multitapering with width equal to two times the fundamental spatial frequency interval and maximum order M equal to 1, 2, or 3. As a reference, the spectra using the Hanning window are included as dotted curves, green for the SeaWinds spectra and black for the model spectra.

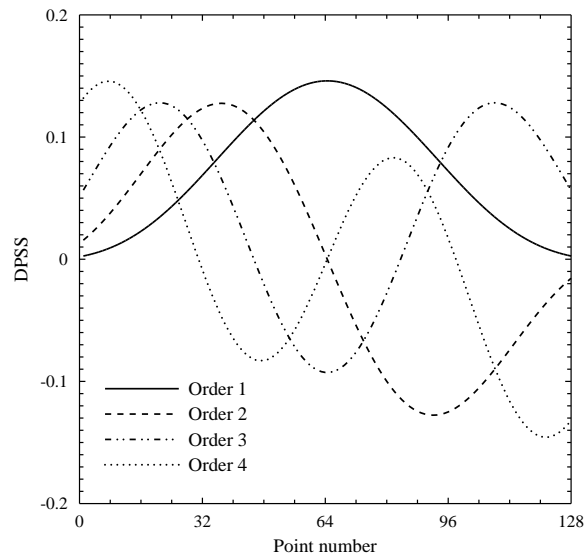


Figure 3.5 Multitaper windows (Discrete Prolate Spheroidal Sequences) with width 2 and order 1 to 4.

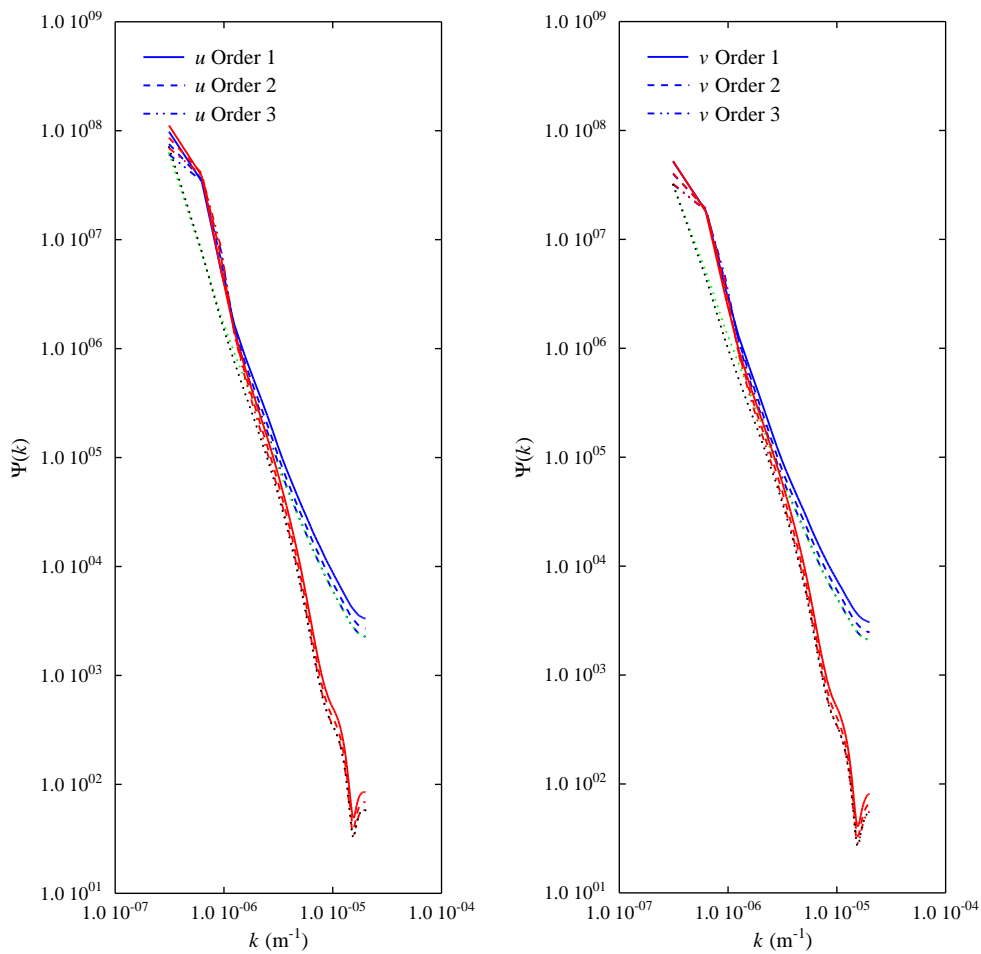


Figure 3.6 Spectra obtained with the multitapering method for width 2 and various orders. The dotted curves show the spectra obtained with Hanning windowing as a reference.

The samples were detrended by applying a Hanning window. The higher order tapering functions are nonzero at the sample ends, as shown in figure 3.5, so without detrending this would result in a discontinuity in the samples, leading to a k^{-2} contribution to the spectrum (no results shown).

At high spatial frequencies the spectra are similar, though there is some vertical shift between them for order 1 and 2. At low frequencies there are considerable differences between the Hanning windowed and the multitaper spectra. As shown by figure 3.6, this is mainly due to overestimation of the variance at low spatial frequencies. The overestimation decreases with increasing order.

The advantage of multitapering is that it minimizes noise in spectra calculated from a small number of samples. The dataset considered here is so large that this advantage does not show up.

3.5 Comparison of the sampling and moments methods

Figure 3.7 shows the spectra obtained with the sampling method (solid lines) and the moments method (dotted lines) for the zonal wind component u and the meridional wind component v . Spectra are shown for the scatterometer winds and the ECMWF background.

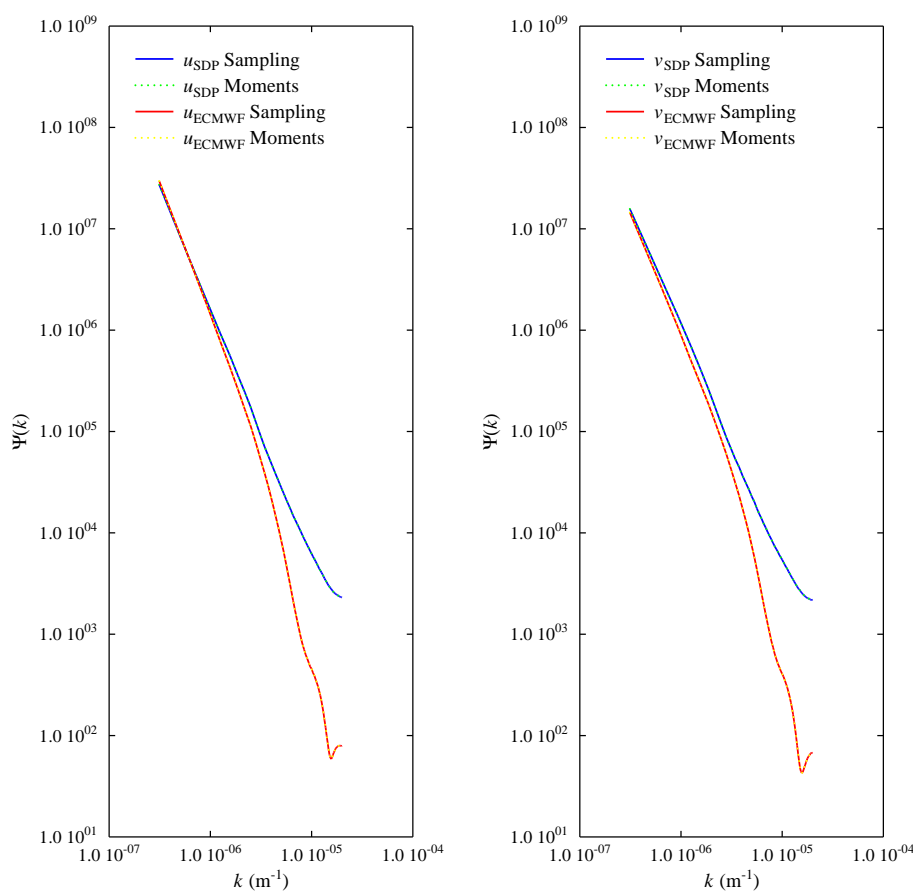


Figure 3.7 Comparison of spectra obtained with the sampling and moments methods with first difference detrending.

The spectra were obtained with first difference detrending. Figure 3.7 shows that the two methods give the same spectrum, and therefore the spectra obtained with the moments method were given a different color. This is as expected, since both methods are shown to be equivalent in sections 2.2 and 2.3.

In order to arrive at the correct normalisation, the sample had to be considered as periodic when calculating the mixed second order moment (so the last point of the sample forms a lag of size 1 with the first point of the sample). In doing so, each point in the sample forms exactly one pair with an other point in the sample at each lag size, see also section 2.3. Moreover, detrending should be applied to the sample before the mixed second order moment is updated

3.6 Sampling strategy

Gap size

So far, isolated missing values have been filled in by linear interpolation (maximum gap size equal to 1) the gap size can be increased or decreased to zero, i.e., no interpolation of missing values applied. Figure 3.8 shows the spectra obtained with gap sizes 0, 1, and 4 using the sampling method with Hanning windowing and sample size 128.

The spectra for gap size 0 and 1 differ only in level while the spectra for gap size 4 show effects of interpolation noise at high spatial frequencies. Table 3.2 shows the statistics for the various values of the maximum gap size. The total number of valid WVC's in the data set equals 25311509. When no interpolation is applied, gap size equal to zero, only 7% of all available valid WVC's is used for calculating the spectra. Interpolating over isolated samples, gap size equal to one, increases the number of WVC's used for calculating spectra to 40% of the total number of valid WVC's. This explains the difference in overall level between the spectra at gap size 0 and 1. Further increment of the gap size has only a small effect on the number of samples, but introduces interpolation noise that adversely affects the spectra at high spatial frequencies.

Gap size	Valid samples	WVC's used for spectra	
0	13918	1781504	7.0 %
1	79094	10124032	40.0%
2	79396	10162688	40.2%
3	79516	10178048	40.2%
4	79586	10187008	40.2%

Table 3.2 Sampling statistics for various values of the maximum gap size.

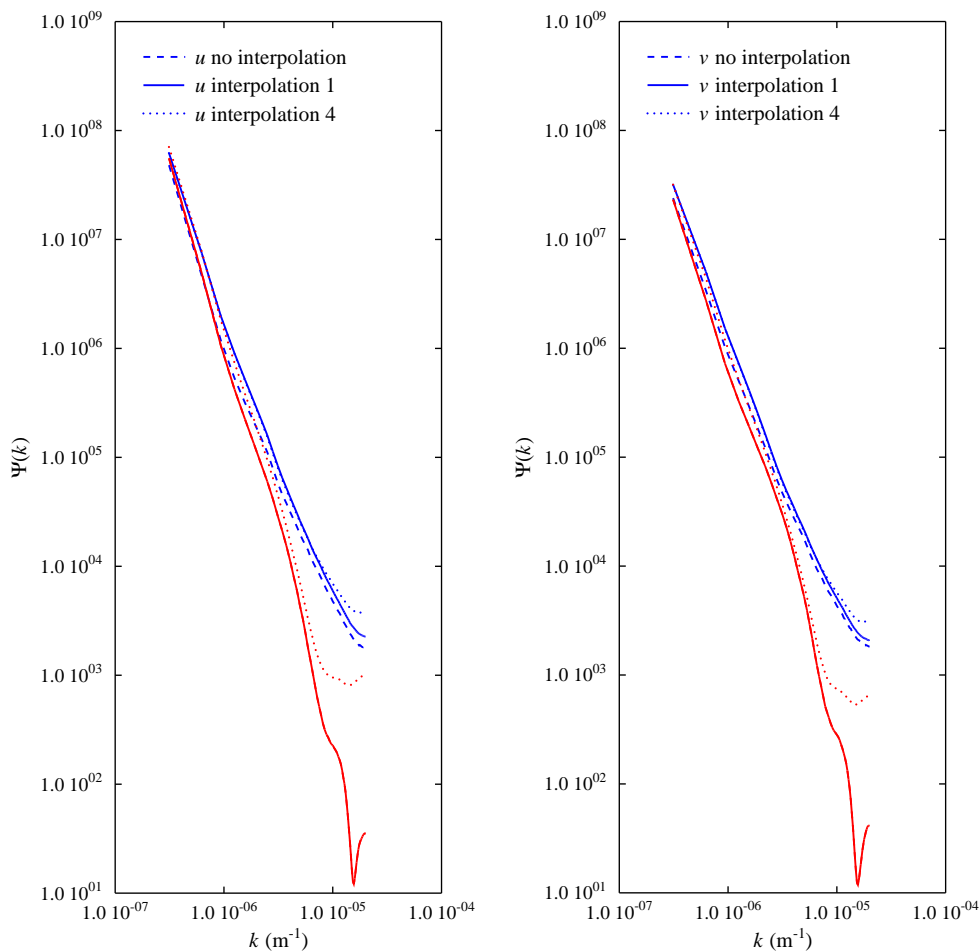


Figure 3.8 Spectra obtained with the sampling method without interpolation and interpolation over isolated missing WVC's.

Figure 3.9 shows the geographic location of the samples for gap size 0 (upper) and gap size 1 (lower). The colours in figure 3.9 indicate the density of sample points, i.e., the number of sample points times 10^5 per square degree. Note the difference in scale between the upper and lower panel .

Without interpolation the samples are more restricted to the open ocean (note the factor 2 difference in scale), in particular the southern Pacific, Atlantic, and Indian Ocean. The sample density in these regions is about twice as large as that for interpolation over isolated points.. When interpolated over isolated missing points also coastal waters contribute. However, as shown in figure 3.8, this has no effect on the shape of the spectrum.

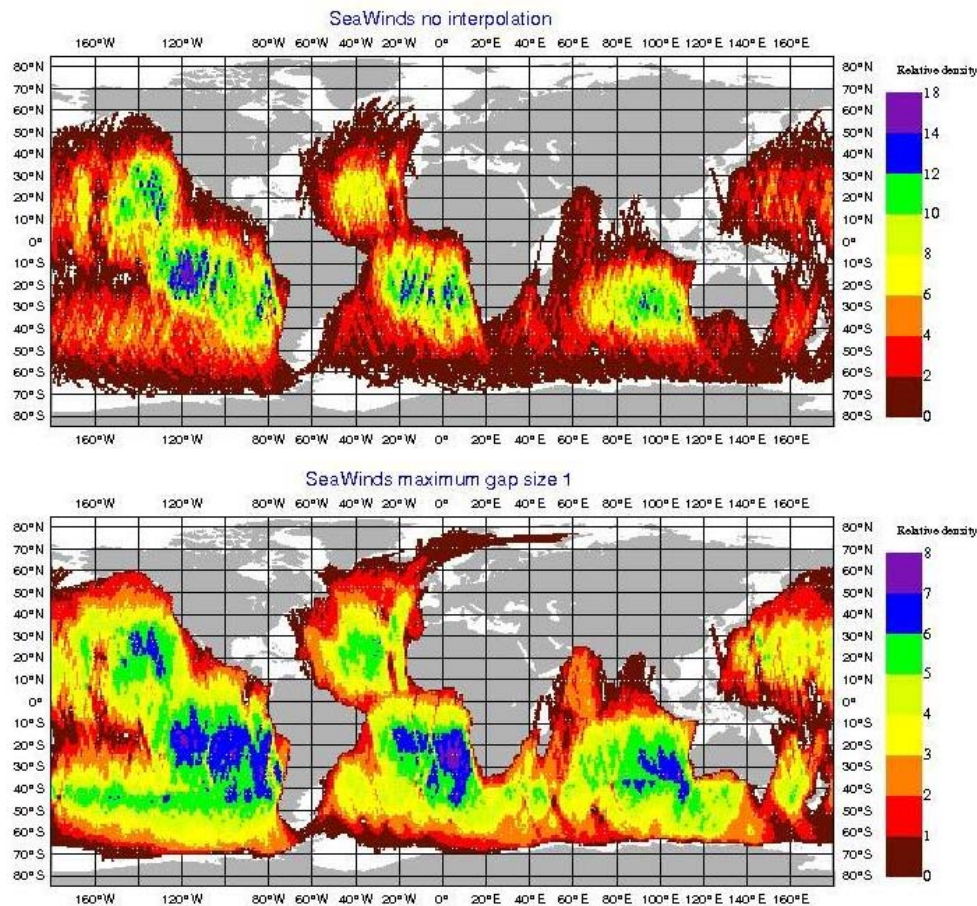


Figure 3.9 Number of sample points times 10^5 per square degree without interpolation (upper) and with interpolation over isolated missing points (lower)

Moments updating

In principle, the moments method has one advantage over the sampling method: when the sample contains missing values, the moments can still be updated for the valid winds only while such a sample must be rejected when using the sampling method. The sampling method is therefore biased to regions without missing scatterometer winds, i.e., regions away from extended rain, sea ice, and land.

In the results shown in figure 3.8 the two methods have been applied to the same samples, i.e., samples without missing values. Figure 3.10 shows the spectra obtained with the moments method using Hanning windowing using the same samples as the sampling method (solid curves) and using all available data (dashed curves).

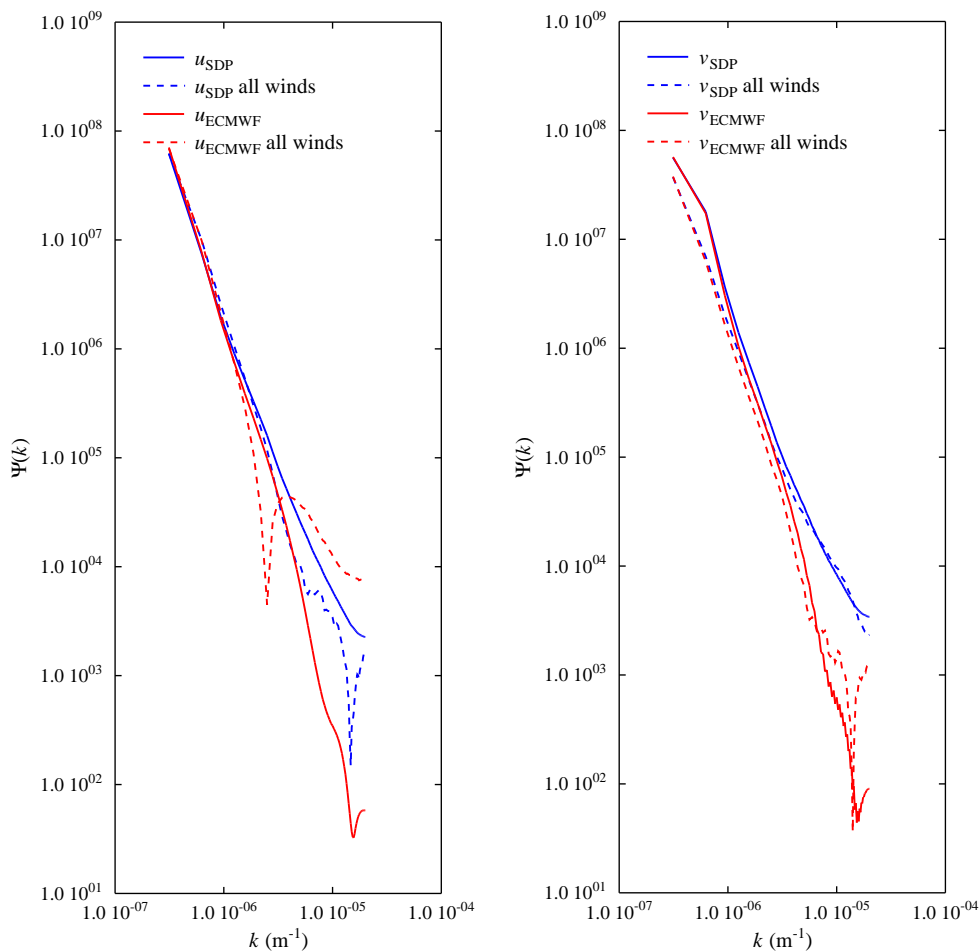


Figure 3.10 Spectra obtained with the moments method using all available samples (solid curves) or all available valid winds (dashed curves) for the wind components u (left) and v (right).

Using all available winds has great effect on the spectrum of the zonal wind component u (left hand panel of figure 3.10). The spectrum of the scatterometer wind using all data (blue dashed curve) is reduced at high spatial frequencies in a manner resembling the model wind spectrum obtained using all valid samples (red solid curve). The spectrum of the model wind obtained using all data (red dashed curve) shows a dip at intermediate spatial frequencies and a strong increase at high spatial frequencies. This spectral behaviour is not consistent with earlier results and is therefore considered as an artefact of the method.

The spectra for the meridional wind component v (right hand panel of figure 3.10) show less difference. Nevertheless, the scatterometer wind spectrum from all data (blue dashed curve) is reduced at low spatial frequencies and exhibits some structure at high spatial frequencies. The model wind spectrum from all data (red dashed curve) shows a similar behaviour.



Sample size

The results so far were obtained for a sample size of 128 (or 129 for first differencing). Table 3.3 shows the number of samples within the data set as a function of the number of points in the sample. Isolated missing points were interpolated over.

First differencing		Other detrending methods	
Sample size	Nr of samples	Sample size	Nr of samples
129	77870	128	79094
257	12598	256	12815
513	220	512	221
1025	0	1024	0

Table 3.3 Number of samples as a function of the sample size for the various detrending methods.

Table 3.3 shows that the number of samples rapidly decreases with the sample size, and that a sample size of 128 is an optimum. Spectra obtained at sample size 128, 256, or 512 show only small differences that may be attributed to an insufficient number of samples for large sample sizes (no results shown).

		How to calculate wind spectra	Doc ID : NWPSAF-KN-TR-008 Version : 1.1 Date : 25-03-2013
--	--	--------------------------------------	---

4 Conclusions

In this chapter report several procedures for calculating the wind spectrum were compared:


- **Detrending**
 - Subtraction method
 - First differencing
 - Windowing
- **Calculation method**
 - Sampling method
 - Moments method
 - Multitapering
- **Sampling strategy**
 - Maximum gap size to be interpolated over
 - All data (moments method only)
 - Sample size

Detrending proves necessary in order to eliminate the effects of a rectangular sampling window leading to a k^{-2} contribution that dominates the spectrum at high spatial frequencies. Detrending with subtraction of a linear transformation mapping the sample ends to zero, first differencing, and windowing give good results. Though there may be substantial differences between the three methods at the lowest spatial frequencies, the spectral densities at medium and high frequencies are the same within 1%.



The wind spectrum obtained as an average over a number of individual spectra (periodograms) does not give the correct variance, because each individual spectrum gives the variance with respect to the average value of that sample, rather than that of the whole dataset. Since the variance is a nonlinear quantity, the averaged variance of all samples is not equal to the variance of the whole dataset. However, since different detrending methods yield almost the same high frequency spectra it is concluded that the detrending methods indicated above give correct spectra.

The sampling and the moments method are identical, as long as the moment method is applied to samples that are considered periodic so that the last point of each sample forms a pair with the first point. Continuous updating of the moments leads to artefacts.

Multitapering may be used for spectral estimates when only a small number of samples is available. The best comparison with Hanning windowed spectra is for maximum order. Multitapering must be used in combination with some detrending method, because the higher order tapering functions are nonzero at the sample edges.



The EUMETSAT Network of Satellite Application Facilities	 NWP SAF Numerical Weather Prediction	How to calculate wind spectra	Doc ID : NWPSAF-KN-TR-008 Version : 1.1 Date : 25-03-2013
---	--	--------------------------------------	---

Interpolation over isolated missing WVC's increases the number of valid samples found in the data set. Further increment of the maximum gap size has little effect. Increasing the sample size leads to a rapid decrease of the number of samples, so a sample size of 128 is considered as optimal.

		<h1>How to calculate wind spectra</h1>	Doc ID : NWPSAF-KN-TR-008 Version : 1.1 Date : 25-03-2013
--	--	--	---

References

- Chelton, D.B., M.H. Freilich, J.M. Sienkiewicz, and J.M. Von Ahn, 2006,
On the use of QuikSCAT scatterometer measurements of surface winds for marine weather prediction. *Mon. Wea. Rev.*, **134**, 2055-2071.
- Errico, R.M., 1985,
Spectra computed from a limited area grid. *Mon. Wea. Rev.*, **113**, 1554-1562.
- Freilich, R. and R. Sharman, 2008,
The use of structure functions and spectra from numerical model output to determine effective model resolution. *Mon. Wea. Rev.*, **136**, 1537-1553.
- Freilich, M.H. and D.B. Chelton, 1986,
Wavenumber spectra of Pacific winds measured by Seasat scatterometer. *J. Phys. Ocean.* **16**, 741-757.
- Patoux, J. and R.A. Brown, 2001,
Spectral analysis of QuikSCAT surface winds and two-dimensional turbulence. *J. Geophys. Res.*, **106D20**, 23,995-24,005.
- Percival, D.B., and A.T. Walden, 1993,
Spectral analysis for physical applications.
Cambridge University Press, Cambridge, New York, USA.
- Press, W.H., B.P. Flannery, S.A. Teukolsky, and W.T. Vetterling, 1988,
Numerical Recipes.
Cambridge University Press, Cambridge, New York, USA.
- Vogelzang, 2006,
On the quality of high resolution wind fields.
Report NWPSAF-KN-TR-002, EUMETSAT, Darmstadt, Germany. (Obtainable from www.metoffice.gov.uk/research/interproj/nwpsaf/scatterometer/OnTheQualityOfHighResolutionWindFields.pdfnwpsaf.org).
- Vogelzang, J., A. Stoffelen, and A. Verhoef,
On the quality of high-resolution scatterometer winds. To be submitted to *J. Geophys. Res.*
- Wikipedia, 2009,
Fourierreeks (in Dutch, no English version of this page found),
<http://nl.wikipedia.org/wiki/Fourierreeks>.

		How to calculate wind spectra	Doc ID : NWPSAF-KN-TR-008 Version : 1.1 Date : 25-03-2013
--	--	--------------------------------------	---

Appendix A Finite differencing

Finite differencing is a technique for mitigating the effects of the trend over a sample. It is treated in chapter 5 of [Percival and Walden, 1993]. However, the full elaboration is left as an exercise, which will be done here.

Let x_t denote the signal sampled on a regular grid $\{t\}$ (which is a wind component in the case of this report). Let the first difference y_t be given by $y_t = x_{t+1} - x_t$. This mapping from x to y can be regarded upon as a filter L defined by

$$y_t = L(x_t) = x_{t+1} - x_t \quad . \quad (\text{A.1})$$

It is easy to show that L is a linear time-invariant filter. Its transfer function $G(f)$ can be calculated from its response to $\exp(2\pi i t f)$

$$L(e^{2\pi i t f}) = e^{2\pi i (t+1) f} - e^{2\pi i t f} = e^{2\pi i j f} (e^{2\pi i f} - 1) = G(f) e^{2\pi i t f} \quad . \quad (\text{A.2})$$

This yields

$$G(f) = e^{2\pi i f} - 1 \quad . \quad (\text{A.3})$$

Suppose that x_t has a spectrum $S_x(f)$ and that y_t has a spectrum $S_y(f)$. According to the theory of linear filtering treated in chapter 5 of [Percival and Walden, 1993], the two spectra are related by

$$S_y(f) = |G(f)|^2 S_x(f) \quad . \quad (\text{A.4})$$

So if the trend is removed by first differencing and the spectrum of the resulting signal is calculated, the original spectrum is retrieved by division by $|G(f)|^2$. Using (A.3), this factor can be written as

$$\begin{aligned} |G(f)|^2 &= (e^{2\pi i f} - 1)(e^{-2\pi i f} - 1) = 1 - e^{2\pi i f} - e^{-2\pi i f} + 1 = \\ &= 2 - (\cos 2\pi f + i \sin 2\pi f) - (\cos 2\pi f - i \sin 2\pi f) = 2 - 2 \cos 2\pi f = \\ &= 2(1 - \cos 2\pi f) = 2(\cos^2 \pi f + \sin^2 \pi f - \cos^2 \pi f + \sin^2 \pi f) = 4 \sin^2 \pi f \quad . \end{aligned} \quad (\text{A.5})$$

So the filter G acts as a high pass filter. Note that $G(0) = 0$, so the spectrum at zero frequency can not be retrieved.

In discrete form we have $f \rightarrow f_k = k / N$, $k = 0, 1, \dots, N/2$ and

$$|G(f_k)|^2 = 4 \sin^2 \left(\frac{\pi k}{N} \right) \quad . \quad (\text{A.6})$$

This equals zero for $k = 1$ and four for $k = N/2$.